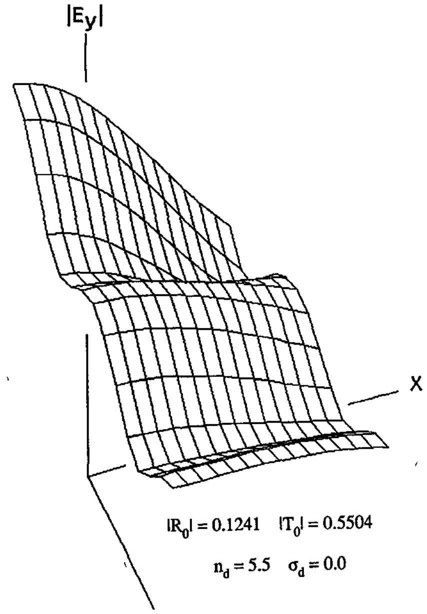


Fig. 12. Spatial variation of total discontinuity region field for large refractive index contrast.

one of the following becomes necessary: distributed feedback, a nonuniform gain profile according to the Bragg diffraction rule, or use of a Fabry–Perot resonator. Moreover, the gain region must be hundreds of wavelengths long, which is computationally prohibitive for the MoM at present.

### Acknowledgment

The authors thank Dr. Herbert Winful of the University of Michigan Optical Sciences Laboratory and Dr. Glen Feak of the University of Michigan Center for High-Frequency Microelectronics for their helpful suggestions.

### References

[1] H. Shigesawa and M. Tsuji, "A new equivalent network method for analyzing discontinuity properties of open dielectric waveguides," *IEEE Trans. Microwave Theory Tech.*, vol. 37, pp. 3–14, Jan. 1989.
[2] E. G. Rawson, "Analysis of scattering from fiber waveguides with irregular core surfaces," *Appl. Opt.*, vol. 13, no. 10, pp. 2370–2377, Oct. 1974.
[3] S. Ray and R. Mittra, "Numerical analysis of open waveguide discontinuities," *Radio Sci.*, vol. 19, no. 5, pp. 1289–1293, Sept.–Oct. 1984.
[4] K. Hirayama and M. Koshiba, "Analysis of discontinuities in an open dielectric slab waveguide by combination of finite and boundary elements," *IEEE Trans. Microwave Theory Tech.*, vol. 37, pp. 761–768, Apr. 1989.
[5] T. G. Livernois and D. P. Nyquist, "Integral-equation formulation for scattering by dielectric discontinuities along open-boundary dielectric waveguides," *J. Opt. Soc. Amer. A*, vol. 4, 1289–1295, 1987.
[6] D. P. Nyquist, D. R. Johnson, and S. V. Hsu, "Orthogonality and amplitude spectrum of radiation modes along open-boundary waveguides," *J. Opt. Soc. Amer.*, vol. 71, pp. 49–54, Jan. 1981.
[7] T. E. Rozzi, "Rigorous analysis of the step discontinuity in a planar dielectric waveguide," *IEEE Trans. Microwave Theory Tech.*, vol. MTT-26, pp. 738–746, Oct. 1978.
[8] B. S. Poh, "Refractive index to gain derivative ratio in GaAs/GaAlAs semiconductor injection lasers," *Proc. Inst. Elect. Eng.*, pt. I, vol. 131, pp. 163–169, Oct. 1984.

# Toward a Unified Efficient Algorithm for Characterizing Planar Periodic Waveguides and Their Applications to MIC and MMIC Circuits

Ké Wu, Pierre Saguet, and André Coumes

***Abstract*—An efficient new algorithm (modified three-dimensional spectral-domain solution with "modal spectrum") applied to a variety of planar waveguides with periodically loaded stubs is achieved. In this paper, slow-wave propagation characteristics and their mechanism of both symmetrically and asymmetrically loaded periodic structures with lossy dielectric layer such as finline and coplanar waveguides (CPW's) are investigated. Using two sets of familiar basis functions, the convergence behavior of the high-speed numerical computation is presented toward a unified efficient algorithm. Many important features such as passband and stopband phenomena related to cutoff and resonant frequencies are discussed in detail based on numerical results, which are compared with measured results obtained by transmission line experimental procedures**

## I. Introduction

With increasing development of millimeter-wave transmission line media and monolithic integrated circuit technologies, there has been growing interest in the properties of hybrid (nonuniform) structures in the transverse section as well as the longitudinal section to realize a more compact package, easier serial implementation, and wider monomode operation. Many planar or quasi-planar waveguides such as finlines and suspended striplines have been suggested and investigated in the frequency range 10 ~ 150 GHz. Little or rather limited information about the nonuniform longitudinal structures has been published, for example, information relating to periodically loaded lines.

On the other hand, coplanar waveguide (CPW) and finline MIS (metal–insulator–semiconductor) structures proposed and analyzed recently by several authors [1]–[5] in an attempt to realize the phase shifters, delay lines, and electronically variable filters make it possible to reduce significantly the component dimensions due to the slow-wave propagation with possible smaller losses. However, the question concerning an efficient slow-wave mode excitation and miniature interconnection of circuits will need to be addressed.

One way to obtain a slow wave is to guide the wave in a direction away from the desired axial direction and to use the axial components. It should be pointed out that a main mechanism of obtaining a slowing down (high $\epsilon_{eff} = (\lambda_{air}/\lambda_{guide})^2$) of propagation is to store the electric and magnetic energy separately in space whether it is transversal or longitudinal. Examples of such structures include the MIS, helix, meander interdig-

Manuscript received March 27, 1987; revised September 17, 1990.
K. Wu was with LEMO-ENSERG, 23 Avenue des Martyrs, BP 257, 38016 Grenoble, France. He is now with the Department of Electrical and Computer Engineering, University of Victoria, PO Box 3055, Victoria, B.C., Canada V8W 3P6.
P. Saguet and A. Coumes are with LEMO-ENSERG, 23 Avenue des Martyrs, BP 257, 38016 Grenoble, France.
IEEE Log Number 9042342.

0018-9480/91/0300-0583$01.00 

ital, and other periodically loaded lines. A number of contributions to classic periodic waveguide and coaxial lines for the application of travelling wave tubes and so on have been published [6], [7] wherein the static field or quasi-TEM conditions were assumed. As early as 1984, only the network analytical method [8] was used to investigate theoretically the passband and stopband properties of single symmetrically loaded periodic stripline and finline. Since then, a new efficient hybrid solution to these structures, being similar to the spectral-domain analysis of periodically nonuniform microstrip lines [9], [10], has been reported together with experimental results [11], [12].

Until now, no detailed studies on slow-wave propagation and cutoff resonance phenomena have been reported related to passband and stopband in these types of structures, especially in asymmetrically and coupled loaded planar waveguides, which have received considerable attention for the application of wider bandwidth couplers and high-quality filters. Accordingly, a full-wave analysis with a comprehensive algorithm is needed for determining the dispersion characteristics.

In this paper, a modified three-dimensional spectral-domain approach is presented in detail to analyze the characteristics of planar periodically loaded structures. It should be noted that a new concept, called modal spectrum, with respect to harmonic waves in the propagation direction is introduced in the analysis; that is, the harmonic wave variation due to the periodic stubs can efficiently be regarded as the natural Fourier development. Consideration of such a fact leads to a considerable alleviation of analytical formulation and numerical computation of the eigen-problems. Specific bidimensional basis functions with completely orthonormal series guarantee fast convergence behavior without spurious solutions. Compared with the method described in [9], [10], this analysis presents an easy-to-read way in which the application of Galerkin's technique becomes more convenient.

Mode propagation in both symmetrically and asymmetrically loaded periodic structures is described and some physical mechanisms are clarified. Slow-wave and loss properties, as well as passband and stopband characteristics, related to the cutoff and resonant frequencies are discussed, and calculated results are compared with measured results.

## II. Theoretical Formulation

Several examples of periodically inhomogeneous suspended stripline and finline with single and coupled stubs in the $H$ and $E$ planes are shown in Figure 1. As demonstrated in [9] and [10], there exist many possible shapes of periodic geometries, for example, triangular and sinusoidal.

In the following, the principle of the modified three-dimensional spectral-domain approach will be demonstrated for two kinds of lossy periodic structures (finline and coplanar waveguide). Although in our analysis only these lines are considered, the theoretical approach can readily be extended to other periodically loaded waveguides. The loss of the dielectric layer is considered because the periodic strip conductors can be placed on a lossy semiconductor (GaAs, Si substrates for examples) in the case of interconnection with other monolithic elements. It is assumed here that the metallization has vanishing thickness, the substrate holding grooves are neglected, and the periodic stubs extend to infinity in the $\pm z$ directions. The theoretical formulation described in detail in [11] leads to

$$\frac{\left(Y_e\alpha^2+Y_h\beta_n^2\right)\tilde{E}_x(\alpha,\zeta_n)}{\alpha^2+\beta_n^2}+\frac{(Y_e-Y_h)\alpha\beta_n\tilde{E}_z(\alpha,\zeta_n)}{\alpha^2+\beta_n^2}=\tilde{J}_x(\alpha,\zeta_n)$$

$$\frac{(Y_h-Y_e)\alpha\beta_n\tilde{E}_x(\alpha,\zeta_n)}{\alpha^2+\beta_n^2}+\frac{\left(Y_e\alpha^2+Y_h\beta_n^2\right)\tilde{E}_z(\alpha,\zeta_n)}{\alpha^2+\beta_n^2}=\tilde{J}_z(\alpha,\zeta_n)$$

where

$$\begin{bmatrix}\tilde{E}_x\\ \tilde{J}_z\\ \tilde{E}_z\\ \tilde{J}_z\end{bmatrix}(\alpha,\zeta_n)=\frac{2}{bp}\iint_S\begin{bmatrix}E_x(x,z)\cos(\alpha x)\\ J_z(x,z)\cos(\alpha x)\\ E_z(x,z)\sin(\alpha x)\\ J_x(x,z)\sin(\alpha x)\end{bmatrix}\exp(j\zeta_n z)\,dx\,dz,$$

$$S\subset\text{aperture}$$

$$\alpha=\frac{(m+0.5K)\pi}{b},\qquad K=\begin{cases}0, & \text{odd mode (electric wall)}\\ 1, & \text{even mode (magnetic wall)}\end{cases}$$

$$\beta_n=\beta_0+\zeta_n,\qquad \zeta_n=\frac{2\pi n}{p}.$$

Here $\beta_0$ is the propagation constant of the dominant harmonic in the Floquet representation, $a$ is the Fourier factor, and $\zeta_n$ represent the higher order harmonics due to the periodically loaded stubs. These could be regarded as the "modal spectrum" in the Fourier sense or the "natural Fourier transform" in a half-periodic cell ($p/2$).

This final formulation (a set of spectral Green's functions) is identical to that of the immittance spectral-domain technique which leads to the final coupled equations by means of a transmission line procedure in the transform coordinates. $Y_e$ and $Y_h$ are the total spectral LSM/LSE immittance at the discontinuity interface [13]. Nevertheless, the field components can be expressed in concrete semianalytical form with this analysis; the advantage of this point consists in the facility of field and power computations.

## III. Numerical Computation

It remains to set bidimensional basis functions for Galerkin's technique, which could be said to be a key step for this method owing to the variational nature of the approach; the efficiency and accuracy of this method depend greatly on the choice of basis functions. The principle of such a choice is to satisfy the boundary conditions and avoid the spurious solutions. Accordingly, a set of completely orthonormal series such as the familiar triangular, Chebyshev, and Legendre functions should be used.

Unlike the network analysis method [8] for the investigation of periodic planar lines, the unknown aperture field can efficiently be divided into two directional field components ($x-z$); also the field quantities are directly expressed in terms of Fourier series. Thus it is more convenient to apply the Galerkin's procedure in this method. In this procedure, the unknown aperture field can be expanded in terms of the appropriate basis functions. Substituting $E_x$ and $E_z$ in the Fourier form as well as $J_x$ and $J_z$ and taking inner products between them, a nontrivial solution for the propagation constant in the periodically loaded structure can be obtained by setting the determinant of the coefficient matrix $M(\beta_0)$ equal to zero:

$$\mathrm{Det}\left[M(\beta_0)\right]=0.$$

Up to this stage, we have to select carefully the basis functions. Two different regions, $S_1$ and $S_2$, are devided corresponding to $s_1\leqslant x\leqslant s_1+w_1$ and $|z|\leqslant p/2$ for $S_1$ and to $s_2\leqslant x\leqslant s_2+w_2$ and $|z|\leqslant d/2$ for $S_2$ (see Fig. 1).

According to the field polarization in the aperture, the basis functions to be used for the TE mode may differ from those for the TM mode. In any case, we can define "guided" basis functions in $S_1$ and "stored" basis functions in $S_2$ by taking $z$-harmonic coupling into account; both terms (guided and stored) refer to the different roles of the two regions. In fact, a transverse resonance should take place in $S_2$, but $S_1$ serves as a channel in which energy is exchanged with the adjacent regions $S_2$ (propagation).

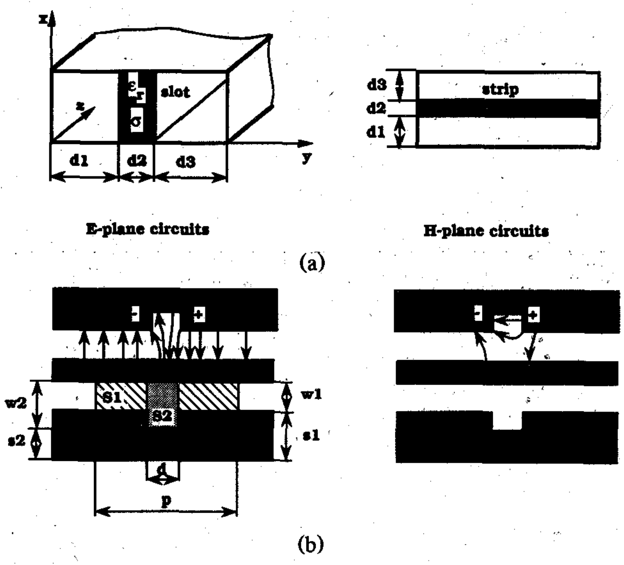


Fig. 1. Illustration of $E$- and $H$-plane circuits for lossy periodic structures. (a) $E$- and $H$-plane configurations of periodic circuits. (b) Electric field patterns of periodic coplanar line (CPW) with arbitrarily located stubs. $S_1$ and $S_2$ are the two subregions in the aperture of a periodic cell.

In this paper, we set the basis functions in two subregions in terms of the multiplication of $f(x)$ and $g(z)$:

$$E_x = \sum_i^{N_{x1}} \sum_j^{N_{z1}} a_{ij}^{\mathrm{I}} f_{xi}^{\mathrm{I}}(x) g_{xj}^{\mathrm{I}}(z) + \sum_i^{N_{x2}} \sum_j^{N_{z2}} a_{ij}^{\mathrm{II}} f_{xi}^{\mathrm{II}}(x) g_{xj}^{\mathrm{II}}(z)$$

$$E_z = \sum_i^{N_{x1}} \sum_j^{N_{z2}} b_{ij}^{\mathrm{I}} f_{zi}^{\mathrm{I}}(x) g_{zj}^{\mathrm{I}}(z) + \sum_i^{N_{x2}} \sum_j^{N_{z2}} b_{ij}^{\mathrm{II}} f_{zi}^{\mathrm{II}}(x) g_{zj}^{\mathrm{II}}(z)$$

where the superscripts I and II denote the subregion represented in the aperture. In both regions, the basis functions can be established as follows. For convenience, a set of familiar triangular functions in consonance with Itoh's argument are used for high-speed computation in seeking an efficient algorithm. With the above considerations in mind, the following set of functions are employed:

$$f_{xi}^{\mathrm{I,II}} = \frac{\cos\left[\dfrac{i\pi(x - s_{1,2})}{w_{1,2}}\right]}{\sqrt{1 - \left[\dfrac{2}{w_{1,2}}(x - s_{1,2}) - 1\right]^2}}, \qquad i = 0, 2, 4, \cdots$$

and

$$\frac{\sin\left[\dfrac{i\pi(x - s_{1,2})}{w_{1,2}}\right]}{\sqrt{1 - \left[\dfrac{2}{w_{1,2}}(x - s_{1,2}) - 1\right]^2}}, \qquad i = 1, 3, 5, \cdots$$

$$f_{zi}^{\mathrm{I,II}} = \frac{\cos\left[\dfrac{i\pi(x - s_{1,2})}{w_{1,2}}\right]}{\sqrt{1 - \left[\dfrac{2}{w_{1,2}}(x - s_{1,2}) - 1\right]^2}}, \qquad i = 1, 3, 5, \cdots$$

and

$$\frac{\sin\left[\dfrac{i\pi(x - 2_{1,2})}{w_{1,2}}\right]}{\sqrt{1 - \left[\dfrac{2}{w_{1,2}}(x - s_{1,2}) - 1\right]^2}}, \qquad i = 2, 4, 6, \cdots.$$

No edge terms $(-1/2)$ are required in the context of functions $g(z)$:

$$g_{xj}^{\mathrm{I}}(z) = g_{zj}^{\mathrm{II}}(z) = \sin\left(\frac{j\pi z}{p}\right)$$

$$\text{for } j = 1, 3, 5, \cdots \quad \text{and} \quad \cos\left(\frac{j\pi z}{p}\right) \quad \text{for } j = 0, 2, 4, \cdots$$

$$g_{xj}^{\mathrm{II}}(z) = g_{zj}^{\mathrm{I}}(z) = \sin\left(\frac{j\pi z}{p}\right)$$

$$\text{for } j = 2, 4, 6, \cdots \quad \text{and} \quad \cos\left(\frac{j\pi z}{p}\right) \quad \text{for } j = 1, 3, 5, \cdots.$$

Obviously, all of basis functions to be described above in the form of complete series are designed to provide an accurate and unified efficient algorithm. On the other hand, they can ensure field continuity when $w_1$ is equal to $w_2$ (uniform case); as such, it means that the "guided" basis functions must be identical to the "stored."

In this way, the bidimensional discontinuity boundary conditions can be treated by a linear combination of such basis functions with an asymptotic property. The choice of basis functions depends not only on the boundary conditions but also on the propagation mode behavior (The TE mode and/or TEM mode for single and coupled slots are dominant along these structures. It is noted that the TM mode should occur only in the resonant state.) This consideration can ensure both magnetic walls at $z = \pm p/2$ and $s_1 < x < s_1 + w_1$.

For the convenience of discussion, numerical results given throughout this paper are obtained for $d_1 = 8$ mm, $d_2 = 0.66$ mm, and $d_3 = 14.2$ mm in WR-90 waveguide with dielectric substrate $\epsilon_r = 2.22$. The fast convergence behavior can be observed by using a low basis function number for most of the cases. We make use of $N_{x1,2} = N_{z1,2} = 2$ and $n = 5$, which may be appropriate in all practical cases.

## IV. Numerical Results and Discussion

The main principle for obtaining a slow wave is to store the electric and magnetic energy separately in space. Thus, MIS (transverse space operation) structures and periodic structures (longitudinal space operation) are employed to generate the slowing down of propagation in a certain frequency range. In this paper, the slow-wave phenomena observed in the passband by both experimental and theoretical analysis could be explained as the coupling of higher order modes in each periodic cell. Note that electric and magnetic fields are concentrated respectively in the smaller slot ($w_1$) and the larger slot ($w_2$).

At and beyond the resonant frequency point, all periodic cells can effectively be regarded as cascaded coupled cavities where the stubs play a significant role.

Fig. 2 illustrates the dispersion characteristics of periodic finlines with arbitrarily located stubs. The comparison between measured and calculated results shows a very good agreement over the passband range, which validates this method. It can be seen that the passband is limited by two points: cutoff and resonant frequencies due to shielded waveguide and periodic stubs. The former seems to be constant (approximately equal to that of the corresponding uniform structure). Indeed, the influence of periodic stubs becomes negligible near the cutoff point.

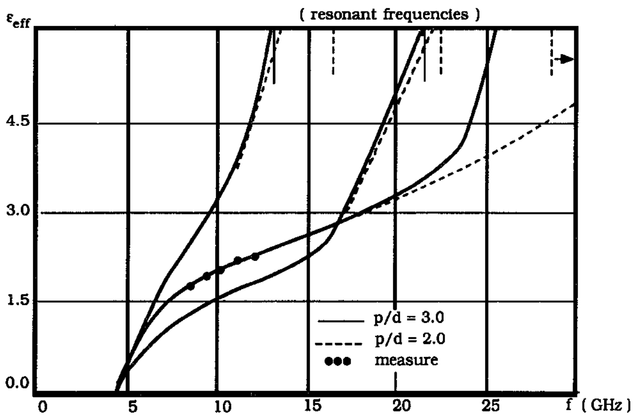


Fig. 2. Dispersion characteristics of periodic finlines with arbitrarily located stubs: $w_1 = 0.5$ mm, $w_2 = 4.5$ mm, $s_1 = 4.83$ mm, $p = 3$ mm.

On the other hand, by moving the stubs from $s_2 = 2.83$ mm (symmetric case) to $s_2 = 4.83$ mm (offset case) the resonant frequency goes down considerably. Another interesting phenomenon is that the resonant frequency can effectively be changed by adjusting the period length without varying the dispersion characteristics over the passband range unless the frequency is in the shadow of resonance.

The resonance phenomenon arises in two cases:

$$s_1 - s_2 = C(2k-1)\lambda/4$$

and/or

$$w_2 - w_1 - s_1 = C(2k-1)\lambda/4$$

$$p = n\lambda/2 \qquad (k, n = 1, 2, 3, \cdots).$$

The coefficient $C$ is determined by geometric conditions. It can easily be seen that the passband and stopband will occur periodically with the frequency.

## V. Conclusion

A new concept called modal spectrum in the propagation direction has been introduced and successfully applied in the theoretical analysis. It makes possible the direct use of the three-dimensional spectral-domain approach in both symmetrically and asymmetrically loaded periodic structures. Several examples based on this unified algorithm illustrate the slow-wave phenomenon as well as passband and stopband behavior related to the cutoff and resonant frequencies. The dielectric losses can be involved.

## References


[1] H. Hasegawa and H. Okizaki, "M.I.S. and Schottky slow-wave coplanar striplines on GaAs substrates," *Electron. Lett.*, vol. 13, pp. 663–664, 1977.

[2] C. M. Krowne, "Slow-wave propagation in generalized cylindrical waveguides loaded with a semiconductor," in *IEEE MTT-S Int. Microwave Symp. Dig.*, 1983, pp. 402–404.

[3] Y. Fukuoda, Y. Shih, and T. Itoh, "Analysis of slow-wave coplanar waveguide for monolithic integrated circuits," *IEEE Trans. Microwave Theory Tech.*, vol. MTT-31, pp. 567–573, 1983.

[4] R. Sorrentino, G. Leuzzi, and A. Silberman, "Characteristics of metal–insulator–semiconductor coplanar waveguides for monolithic microwave circuits," *IEEE Trans. Microwave Theory Tech.*, vol. MTT-32, pp. 410–415, 1984.

[5] A. Abdel Azeim, H. El Hennawy, and S. Mahrous, "Analysis of finlines on semiconductor substrate," in *Proc. 14th European Microwave Conf.* (Liege, Belgium), 1984, pp. 346–351.

[6] R. M. Bevensee, *Electromagnetic Slow-Wave System.* New York: Wiley, 1964.

[7] L. U. Field, "Some slow-wave structures for travelling waves tubes," *Proc. IRE*, vol. 37, no. 1, pp. 34–40, 1949.

[8] T. Kitazawa and R. Mittra, "An investigation of strip lines and finlines with periodic stubs," *IEEE Trans. Microwave Theory Tech.*, vol. MTT-32, pp. 686–688, 1984.

[9] F. J. Glandorf and I. Wolf, "A spectral domain hybrid field analysis of periodically inhomogeneous microstrip lines," in *IEEE MTT-S Int. Microwave Symp. Dig.*, 1984, pp. 466–469.

[10] F. J. Glandorf and I. Wolf, "A spectral domain analysis of periodically nonhomogeneous microstrip lines," *IEEE Trans. Microwave Theory Tech.*, vol. MTT-35, pp. 336–343, 1987.

[11] K. Wu, V. Dzougaiev, and P. Saguet, "A complete theoretical and experimental analysis on properties of periodic planar structures," *Proc. Inst. Elec. Eng.*, vol. 135, pt. H, No. 1, Feb. 1988.

[12] V. Dzougaiev, K. Wu, and P. Saguet, "Experimental and theoretical investigation of characteristics of periodic-loaded finlines," *Electron. Lett.*, vol. 22, pp. 984–985, 1986.

[13] T. Itoh, "Spectral domain immittance approach for dispersion characteristics of generalized printed transmission lines." *IEEE Trans. Microwave Theory Tech.*, vol MTT-28, pp. 733–736, 1980.


# On the Calculation of Conductor Loss on Planar Transmission Lines Assuming Zero Strip Thickness

Peter Heitkämper and Wolfgang Heinrich

*Abstract* —**The incompatibility of the zero-strip-thickness assumption with conductor loss calculation based on the common perturbation approach is addressed. Numerical results are shown that demonstrate the unbounded behaviour of the attenuation constant in this case. This observation is of specific interest because it applies to various data on loss given in the literature.**

## I. The Problem

Conductor loss on planar transmission lines such as microstrip, coplanar waveguide, and slotline is usually calculated by means of a perturbation approach. One starts from an analysis of the lossless waveguide and then determines the attenuation from the corresponding surface currents on the conductors. Assuming the tangential magnetic field to remain approximately unchanged by the losses, one arrives at the well-known formula

$$P_c = \frac{1}{2} R_s \int_C |\vec{H}_t|^2 \cdot ds \tag{1}$$

where $P_c$ denotes the dissipated power per unit length, $R_s$ the surface resistance of the conductors, $\vec{H}_t$ the tangential magnetic field, and $C$ the integration path along the contour of the conductors. Consequently, for the attenuation constant $\alpha_c$ caused by the conductor losses, one has

$$\alpha_c = \frac{1}{2} \cdot \frac{P_c}{P_z} \tag{2}$$

with $P_z$ being the total power transported in the longitudinal direction along the waveguide. Clearly, such a procedure makes

Manuscript received July 11, 1990; revised November 21, 1990.

P. Heitkämper is with the Institut für Netzwerk- und Signaltheorie, Technische Hochschule Darmstadt, Merckstrasse 25, D-6100 Darmstadt, Germany.

W. Heinrich is with the Institut für Hochfrequenztechnik, Technische Hochschule Darmstadt, Merckstrasse 25, D-6100 Darmstadt, Germany.

IEEE Log Number 9042354.

0018-9480/91/0300-0586$01.00 ©1991 IEEE